

Volume Grain Analysis in Organic Thin Film Semiconductors

T. Gredig*, D. Bergman, K. P. Gentry

Department of Physics & Astronomy, California State University Long Beach,
1250 Bellflower Blvd., Long Beach, CA 90840-3901, USA

*tgredig@csulb.edu

ABSTRACT

The grain structure of organic thin films is quantitatively studied using atomic force microscopy images. The grain morphology affects the charge transport of organic polycrystalline thin film devices due to charges at grain boundaries. Thus, the grain growth plays a crucial role for the optimization of organic thin film devices. Iron phthalocyanine, a planar small molecule, is thermally evaporated and grain distributions for thin films are measured. The nominal grain size diameter can be controlled between 30 - 200 nm for samples deposited between room temperature and 260 °C. The phthalocyanine grains are elongated and can be approximated by an ellipsoid. The grain size distributions are analyzed with a watershed algorithm that provides the grain area and volume. The grain volume distribution can be fit to a lognormal distribution. The minor and major axes distribution of the areal ellipse differ and best fit a normal and lognormal distribution, respectively. The anisotropic growth is attributed to the asymmetry of the small molecule.

Keywords: grain size distribution, atomic force microscopy, phthalocyanine, morphology, thin film, grain volume

1 INTRODUCTION

Polycrystalline organic thin films have many technological applications, such as gas sensors, flexible photovoltaics, and organic light emitting diodes.[1] Recent advances have shown that the charge transport of organic semiconductors shows a variety of new concepts due to the interaction of the π -electronic structure and its thin film morphology.[2]–[4] Therefore, a quantitative understanding of the film growth and grain structure is pertinent to improve device fabrication. Furthermore, it allows for a better understanding of intrinsic characteristics such as bias stress, trap levels, defects, adsorption rates and other properties of π -conjugated materials. In organic field-effect transistors the first monolayers form the charge transport channel.[5] Recently, quantitative analyses using atomic force microscopy in pentacene thin films have shown diffusion limited aggregation for the growth of the first few layers.[6] Also,

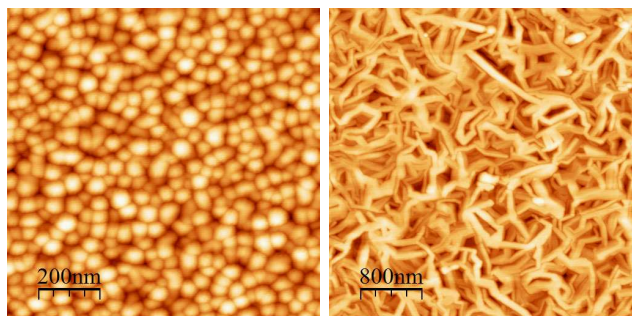


Figure 1: Atomic force microscopy images for iron phthalocyanine thin films deposited at room temperature (left) and 200 °C (right). The $1 \times 1 \mu\text{m}^2$ image shows small rounded grains at room temperature, whereas the $4 \times 4 \mu\text{m}^2$ image shows elongated grains growing in random directions at high deposition temperatures.

polycrystalline silicon films can be fabricated by thermal annealing from amorphous precursors. The crystallite area distributions are measured with transmission electron microscopy and reveal lognormal-like distributions.[7] This process can be understood with a random nucleation and growth model and yields analytical solutions for kinetics and grain size distributions.[8], [9] Such models and simulations provide important insight in the time-dependent growth process. Yet, these examples and most other experimental data are limited to two-dimensional grain area distributions ignoring the full details of the crystallite structure. From a theoretical point of view, important model and simulation verification comes from the precise three-dimensional structure.[10] In the following a quantitative analysis of the three-dimensional grain volume of phthalocyanine thin films is presented based on an atomic force microscopy analysis that includes height information.

2 EXPERIMENT

In order to study grain size distributions, thin films of iron phthalocyanine (FePc) were deposited by thermal evaporation in vacuum. Metallo-phthalocyanines ($\text{M-C}_{32}\text{N}_8\text{H}_{16}$) are the archetype of planar and π -conjugated small molecules.[11] The base pressure of the evaporation chamber was below $7 \cdot 10^{-7}$ mbar. The FePc powder

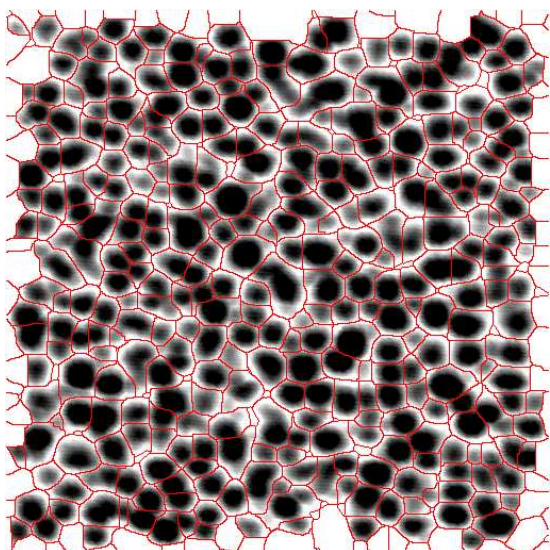


Figure 2: Watershed processed atomic force microscopy image of an iron phthalocyanine thin film deposited at room temperature. The image is $1 \times 1 \mu\text{m}^2$ in size. The partial edge grains are removed from the statistics using the information from the bounding box. The height information from the original AFM image is used to infer the grain volume for each grain outlined in the image.

was purchased from Sigma-Aldrich and then purified in three cycles using a thermal gradient vacuum tube furnace. The substrate surface is carefully cleaned before all depositions. The deposition rate was between 0.3 and 0.4 Å/s. X-ray diffraction data of the FePc thin films show a pronounced peak at $2\theta = 6.8^\circ$ for films deposited on both silicon and sapphire substrates and confirm the polycrystalline nature of the thin film.[12] In particular, the (200) peak indicates that the plane of the FePc molecule is perpendicular to the substrate surface; i.e. the unit cell's b-axis is parallel to the substrate.[13] The thin films are subsequently analyzed using atomic force microscopy (AFM) employing a NanoScope III MultiMode™ in tapping mode.[14]

3 RESULTS

The grain size and surface morphology of FePc thin films are strongly influenced by the deposition temperature. From the atomic force microscopy images, small rounded grains are measured in samples deposited at room temperature (Fig. 1). The nominal grain size diameter ranges from 20 - 50 nm and only a small asymmetry is apparent. However, it should be noted that the stacking order implies that the major axis contains four to five times more molecules as compared to the minor axis. This is due to the planarity of the molecule. At elevated deposition temperatures, the grain size dramatically increases for nominally equal films as shown

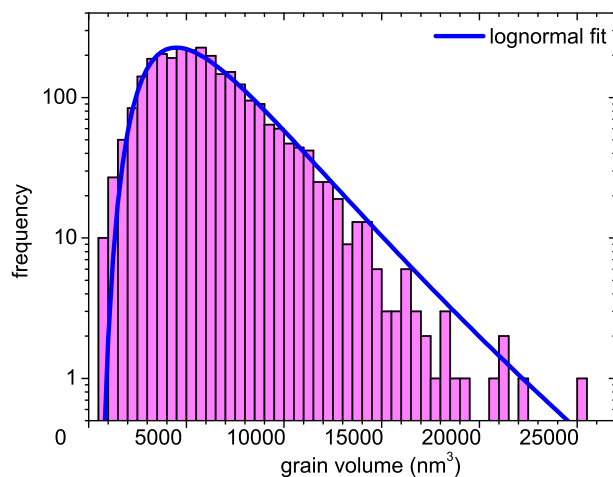


Figure 3: The grain volume is plotted for an iron phthalocyanine thin deposited at room temperature. The distribution is fit with three parameters to the lognormal function (line), where the mean is 5676 nm^3 and the standard deviation 0.49.

in Fig. 1. The mean grain size increases by almost one order of magnitude such that there are 650 molecules on average in a grain along the major axis and 70 molecules along the minor axis. The shape of the grain is strongly elliptical, as the major axis grows much faster than the minor axis with deposition temperature. From the line trace of the atomic force microscopy image, individual plateaux appear that are spaced 1.3 nm corresponding to the molecule's size.[15]

Since the resolution of atomic force microscopy (AFM) images generally limits the number of grains to at most a few hundred per image, several AFM images were combined to produce statistics of several thousand grains. The grain boundaries are determined with a watershed algorithm[16] and partial grains at the edge of the image are removed from the analysis, see Fig. 2. For each grain, the perimeter, area, and bounding or Zingg box are determined to build distributions. Using the explicit AFM height information, each grain is integrated over its area to sum up the total grain volume under the assumption that no smaller grains are hidden underneath. This assumption appears to be mostly true for thin films with the thickness less than the mean grain size diameter. It should be noted that the grain volume is systematically overestimated due to the finite AFM cantilever tip size and the tip-sample interaction. In this fashion, the distribution of more than 2200 grains for an iron phthalocyanine thin film deposited at room temperature is summarized in Fig. 3. The lognormal distribution has a lower reduced χ^2 of 86 compared to 211 for a best fit to a normal distribution. The asymmetry of the grains is further analyzed by fitting an ellipse of equal area to each grain. The major axis has a

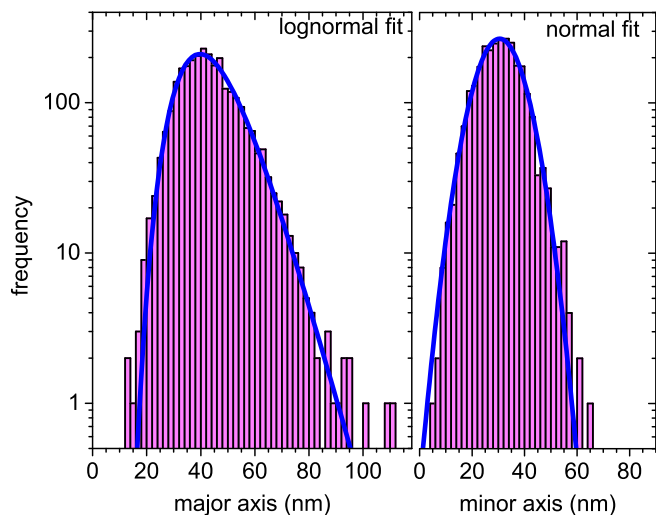


Figure 4: The grain is fit to an ellipse and the distributions of the major and minor axis are fit with 3 parameters each. The lognormal distribution describes the major axis length better and yields a mean of 42.3 nm and a standard deviation $\sigma = 0.25$. For the minor axis a normal distribution has a lower reduced χ^2 value with a mean of 30.5 nm and a distribution width of $\sigma = 16.5$ nm.

mean value of 42 nm versus the minor axis length, which is only 30 nm. However, the circularity decreases dramatically with deposition temperature as more kinetic energy allows the molecules to diffuse farther and form longer chains evolving into the characteristic needle-like shapes seen in micrographs.

The separated distributions of the major and minor axes differ; the major axis fits better to the lognormal distribution, whereas the minor axis grain distribution has a lower reduced χ^2 for the normal distribution as demonstrated in Fig. 4. This is evidence for the asymmetric growth of grains and crystallites in phthalocyanine thin films.

4 CONCLUSIONS

The distributions of iron phthalocyanine grains of polycrystalline thin films are studied quantitatively. A watershed-based algorithm is employed to determine grain boundaries of atomic force microscopy images. The AFM height information is integrated to determine not only the grain area, but importantly the grain volume. In a simple model, the grains are evaluated as ellipsoids having three axes. The major and minor axis in the plane are best described with a lognormal and normal grain distribution respectively. The grain volume fits well the lognormal distribution. This analysis provides detailed experimental data to improve the understanding of grain growth, grain boundaries, and volume.

5 ACKNOWLEDGEMENTS

This research was supported by the National Science Foundation in the Division of Materials Research (Grant No. DMR-0847552) and the Undergraduate Research Provost Award at the California State University, Long Beach. The authors would like to thank Dr. José de la Venta for performing x-ray diffraction measurements and Prof. Andreas Bill for many insightful discussions.

REFERENCES

- [1] R. D. Yang, T. Gredig, C. N. Colesniuc, J. Park, I. K. Schuller, W. C. Trogler, and A. C. Kummel, *Appl. Phys. Lett.* **90**, 263506 (2007).
- [2] V. Coropceanu, J. Cornil, D. A. da Silva Filho, Y. Olivier, R. Silbey, and J.-L. Brédas, *Chem. Rev.* **107**, 926 (2007).
- [3] J. Locklin and Z. Bao, *Anal. Bioanal. Chem.* **384**, 336 (2006).
- [4] T. Gredig, I. N. Krivorotov, and E. D. Dahlberg, *Phys. Rev. B* **74**, 094431 (2006).
- [5] G. Horowitz, *Adv. Mat.* **10**, 366 (1998).
- [6] B. Stadlober, U. Haas, H. Maresch, and A. Haase, *Phys. Rev. B* **74**, 165302 (2006).
- [7] R. B. Bergmann, F. G. Shi, H. J. Queisser, and J. Krinke, *App. Surf. Sci.* **123-124**, 376 (1998).
- [8] R. B. Bergmann and A. Bill, *J. Cryst. Growth* **310**, 3135 (2008).
- [9] A. V. Teran, A. Bill, and R. B. Bergmann, *Phys. Rev. B* **81**, 075319 (2010).
- [10] M. Hillert, *Mat. Sci. Forum* **204-206**, 3 (1996).
- [11] T. Gredig, K. P. Gentry, C. N. Colesniuc, and I. K. Schuller, *J. Mat. Sci.* **ICAM 2009**, 1573 (2010).
- [12] G. Liu, T. Gredig, and I. K. Schuller, *Europhys. Lett.* **83**, 56001 (2008).
- [13] H. Peisert, T. Schwieger, J. M. Auerhammer, M. Knupfer, M. S. Golden, J. Fink, P. R. Bressler, and M. Mast, *J. Appl. Phys.* **90**, 466 (2001).
- [14] I. Horcas, R. Fernández, J. M. Gómez-Rodríguez, J. Colchero, J. Gómez-Herrero, and A. M. Baro, *Rev. Sci. Instr.* **78**, 013705 (2007).
- [15] K. P. Gentry, T. Gredig, and I. K. Schuller, *Phys. Rev. B* **80**, 174118 (2009).
- [16] L. Vincent and P. Soille, *IEEE Trans. Patt. Anal. Mach. Intel.* **13**, 583 (1991).